Chapter

Building and Architecture Paints and Coatings

Valentina Loganina and Yerkebulan Mazhitov

Abstract

Information is given on the strength of the coatings of cement concrete for the exterior walls of buildings. It was found that the strength of the coating depends on the quality of its appearance. A strength model is proposed depending on the surface roughness of the coating. The influence of the scale factor on the change in the strength of coatings is established. To assess the long-term strength of the coatings, we studied the temperature-time dependence of strength. The values of the activation energy of the destruction process of some coatings are experimentally determined. The dependence of the long-term strength of the coatings on tensions is given. The kinetics of changes in the short-term strength of coatings during aging is considered from the perspective of the kinetic concept of the strength of solids. The condition for coating cracking is obtained. Taking into account the influence of the scale factor and the conditions of brittle fracture of coatings, a method for choosing the optimal coating thickness is proposed.

Keywords: coatings, structure, properties, coating strength, coating appearance quality, mathematical model of strength

1. Introduction

Construction and maintenance of buildings and structures require a large number of paints. The share of building paints and varnishes, including repair materials, accounts for up to 5–55% of the total volume of manufactured paints and varnishes, of which 46–48% are paints and 5–8% are varnishes. The main market share of coatings is architectural and decorative coatings.

Currently, for the decoration of building facades, compositions based on polymer binders are widely used: water-dispersion, perchlorovinyl, organosilicon, polymer-cement, silicate paint, sol silicate, and polymer silicate paint [1–3]. The proportion of organosoluble products in the total consumer market of paints and varnishes has now stabilized at about 15%, and the share of water-dispersion varnishes and paints is more than 60%.

The problem of reliability and durability of protective and decorative coatings of the exterior walls of buildings is one of the urgent scientific and technical problems in the field of materials science [4, 5]. It is known that the durability of coatings depends on the type of binder, the technology of applying the paint composition, operating conditions, etc. [6–8].

Crack resistance is the main characteristic that characterizes the durability of finishing coatings. The main reasons for the occurrence of cracks are significant

shrinkage deformations that occur during the hardening of finishing coatings as well as during operation. The property values of the coats on a cement backing are known to be variable and depend on a number of factors (the roughness and porosity of the backing, technological factors, etc.) [9, 10]. However, at present, many issues of strength and durability of coatings of cement concrete are not considered.

2. Strength of protective and decorative coatings

One of the most common types of destruction of coatings is cracking and peeling [11]. Coating cracking occurs when internal tensile stresses reach the cohesive strength of the coating material, i.e.,

$$\sigma = \mathrm{R\,kog} \tag{1}$$

Thus, to assess the resistance of coatings to cracking, it is necessary to identify patterns of change in the strength of coatings.

The presence of defects on the surface of coatings will undoubtedly affect the physicomechanical properties of coatings.

The probability of destruction of protective and decorative coatings depending on the presence of defects on their surface can be defined by the formula:

$$P = 1 - e^{-\rho S} \tag{2}$$

where p is the defect concentration and S is the surface area.

As can be seen from formula (2), for the same surface area S, the probability of coating failure increases with increasing defect concentration [8].

In the study the following paint is used: alkyd enamel PF-115 grade, polystyrene paint brands PS-160, silicone enamel KO-168, polyvinyl acetate cement (PVAC) paint, silicate paint, polymer-lime paint, lime paint, and perchlorovinyl XB-161.

The surface roughness of the paintwork was evaluated which is determined by profilograph TR-100 [12].

Assessment deformation of coating was carried out with the help of a tensile machine IR 5057–50 with the samples after 28 days of curing. The method is based on the sample stretching until it ruptures (deformation speed of 1 mm/minute).

The $1 \times 1 \times 5$ cm samples were fixed in the clips of the tensile machine so that their longitudinal axis was in the direction of stretching and the force was applied equally all over the sample section. The tests were carried out at the temperature of 20°C and relative air humidity of 60%. The ultimate tensile strength estimation was carried out for not less than four samples of each compound. The ultimate tensile strength R_{kog} for each sample is derived from the formula:

$$R_{\mathrm{kog}} = \frac{F_{Pi}}{S_{Oi}} \tag{3}$$

where F_{Pi} is the stretching loading at the time of a rupture, N, and S_{Oi} is the initial cross-sectional area of a sample, mm^2.

The modulus of elasticity was calculated according to the chart "tension deformation" on an inclination tangent of angle to abscissa axis of the tangent, which was drawn to an initial straight section of the chart.

The modulus of elasticity for each sample (E_{upr}) in MPa is derived from the formula:

$$E_{upr} = \frac{R'_{kogi}}{\varepsilon'_i} \cdot 100 \quad (4)$$

where R'_{kogi} is the ultimate tensile strength at the time of the tangent separation from the chart "tension deformation," MPa, and ε'_i is the relative lengthening at the time of rupture, %.

The presence of defects on the surface of the coatings will undoubtedly affect the physicomechanical properties of paint coatings. It is revealed that the elastoplastic character of the destruction is characteristic for the coatings studied.

Regardless of the type of paint composition, the strength and relative deformations are reduced, the plastic deformation is increased, and the elastic surfaces are reduced with increasing roughness (**Figures 1–4**) [13]. Thus, when the surface of coating roughness based on paint PS-160 is Ra = 0.74 μm, the tensile strength R_p is 69.4 kgf/cm^2, the relative strain ε = 3.1%, and with a roughness Ra = 0.86 μm - R_p =

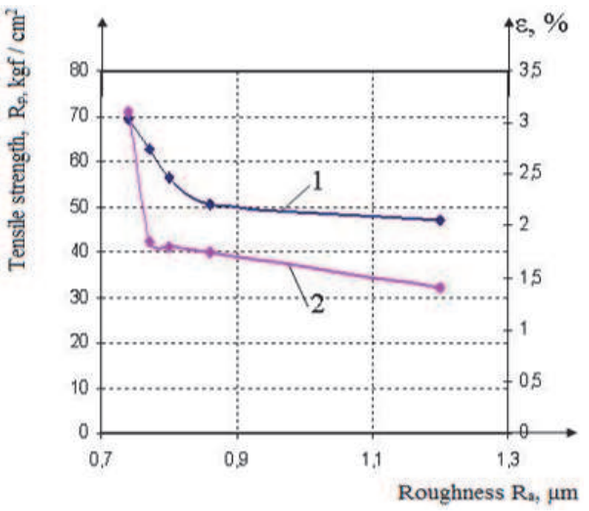

Figure 1.
Dependence of the tensile strength (1) and the relative elongation (2) on the roughness of the film surface based on paint PS-160.

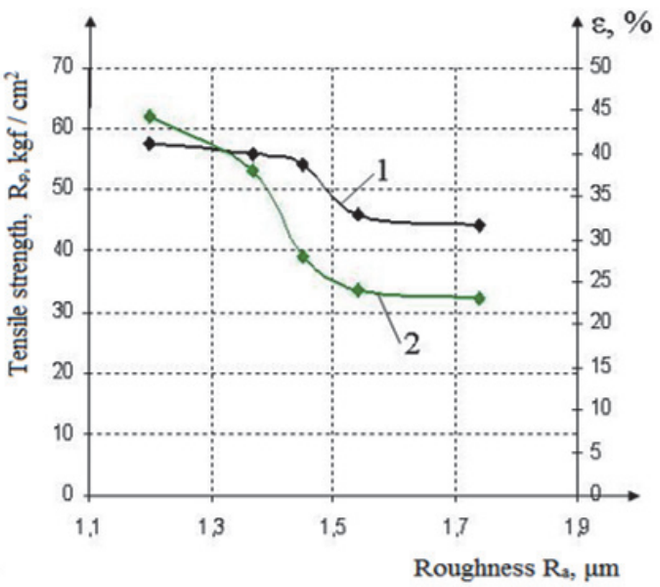

Figure 2.
Dependence of the tensile strength (1) and the relative elongation (2) on the roughness of the film surface on based of paint PF-115.

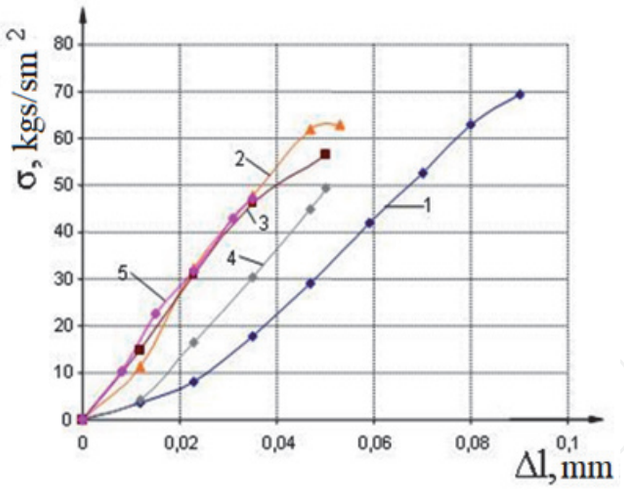

Figure 3.
Tensile diagrams of films based on PS paint, 160: (1) roughness of 0.74 μm; (2) roughness of 0.77 microns; (3) roughness of 0.8 microns; (4) roughness of 0.86 microns; (5) roughness 1.2 μm.

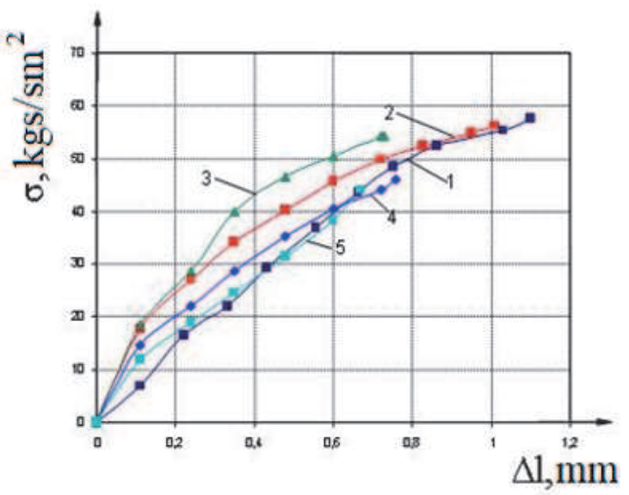

Figure 4.
Tension diagrams of films based on PF paint, 115: (1) roughness 1.2 μm; (2) roughness of 1.37 μm; (3) roughness of 1.45 μm; (4) roughness of 1.54 microns; (5) roughness of 1.74 μm.

50.5 kgf/cm^2 and 1.75%, respectively. At a roughness of the film based on the paint PF-115 Ra = 0.74 μm, the tensile strength R_p is 57.7 kgf/cm^2, and the relative strain ε = 44.3%, at a roughness Ra = 1.74 μm - R_p = 44.1 kgf/cm^2 and 23%, respectively.

For films on the basis of the investigated paint, the flowing character of the curve "tensile strength-roughness" with a sharp decline in strength to a certain value is observed, constituting 45–55 kg/cm^2 at the roughness of the film, respectively, on the basis of the paint PF-115 (1.4–1.6 micrometers) and on the basis of the paint PS-160 (0.8–1 microns). With further increase in the roughness of the film surface, at least a significant reduction in tensile strength is observed.

Analysis of the data shown in **Figures 1** and **2** shows that the dependence of the tensile strength on the roughness of the surface of the films can be approximated by an expression of the form

$$R_p = a \cdot e^{b \cdot R_a} \tag{5}$$

where R_a is the surface roughness, μm; b is the coefficient that takes into account the degree of reduction in strength from roughness, μm^{-1}; and a is the coefficient that characterizes the value of tensile strength, at R_a = 0 (ideal model).

For films based on PS-160 paint, model (5) has the form

$$R_p = 110.5 \cdot e^{-0.761 \cdot R_a} \tag{6}$$

For films based on PF-115 paint,

$$R_p = 114.5 \cdot e^{-0.548 \cdot R_a} \tag{7}$$

The presented models make it possible to evaluate the expected tensile strength depending on the surface roughness of the coatings.

The influence of the scale factor on the tensile stress of the films is revealed. **Figures 5** and **6** show the results of a study of the effect of film thickness on a change in tensile strength of PVAC and silicate of the coating.

An analysis of the data shows in **Figure 5** that an increase in the thickness of liquid glass-based films from 0.16 to 0.52 mm leads to a decrease in tensile strength from 9.44 to 5.56 MPa, respectively. Similar patterns are also characteristic of films based on a mixture of water glass and styrene acrylic dispersion.

An analysis of the data obtained (**Figures 5** and **6**) shows that the dependence of the tensile strength on the film thickness can be approximated by the expression

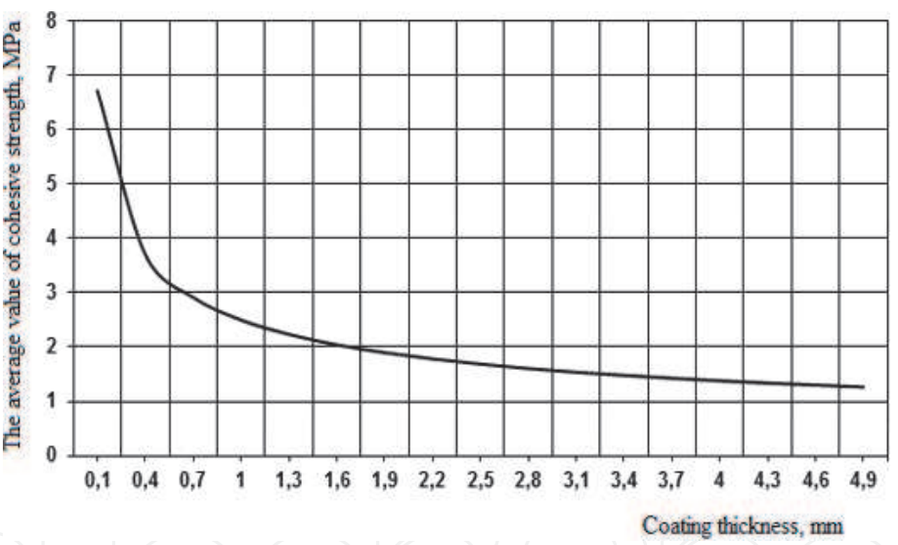

Figure 5.
Dependence of cohesive strength of PVAC coatings on their thickness.

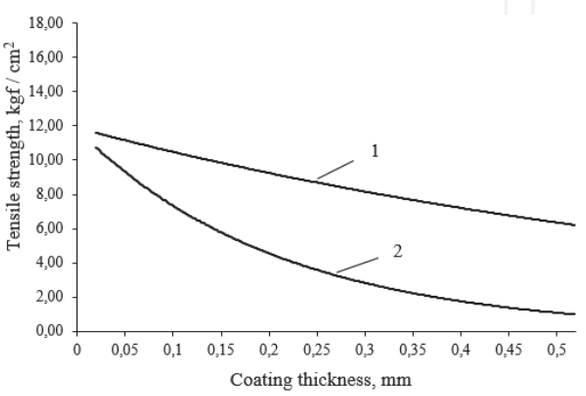

Figure 6.
Dependence of cohesive strength on film thickness: (1) based on silicate paint; (2) based on polymer silicate paint.

$$R_p = Ah^b \tag{8}$$

where h is the film thickness.

Mathematical data processing (curves 1 and 2, **Figure 6**) showed that they are well described by the expression:

For silicate-based films

$$R_p = 5.030h^{-0.37} \tag{9}$$

For films based on polymer silicate paint

$$R_p = 0.886h^{-1.3} \tag{10}$$

The correctness of the equations was checked by Fisher's criterion.

3. Development of sol silicate paint

Sol silicate paint were used a filler microcalcite MK-2 (TU 09 5743-001-91892010-2011) and talc MT-GShM (GOST 19284-79) and a pigment titanium dioxide 230 rutile form (TU 2321-001-1754-7702-2014), ocher (GOST 8019-71), iron red oxide (GOST 8135-74), ultramarine UM-1 (OST 6-10 - 404 - 77), and chromium oxide OHP-1 (GOST 2912-79). To determine the content of the pigment (filler), the viscosity was measured using a viscometer VZ-4. To obtain different shades, titanium dioxide is mixed with an appropriate pigment [14].

Figure 7 shows the dependence of viscosity of paint on the content of pigment and filler. As can be seen from the obtained data, when filling in the range of about $0 < \varphi < 0.12$, the viscosity increase is insignificant, and the polymer matrix only partially passes into the film state. With a low concentration of pigment (filler), the boundary layers of distant particles do not constitute an independent phase in the bulk of the material that can influence its properties. With further filling ($\varphi > 0.12$), there is a significant change in the ratio of bulk and film phases of the matrix, and a sharp increase in the viscosity of the composition is observed.

In **Figure 8** the dependence of viscosity on the volume fraction of pigment in the coordinates lg□ - C (where C is the concentration of pigment and filler in the system) is shown. This dependence consists of two intersecting straight lines.

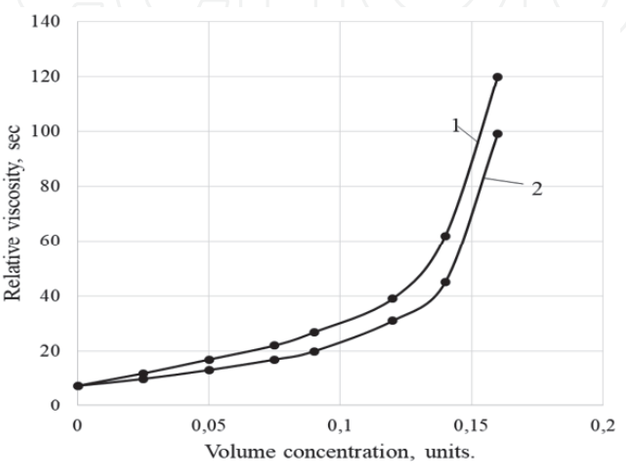

Figure 7.
The dependence of the viscosity of the sol of silicate paint on the content of pigment and filler: (1) sol silicate paint; (2) sol silicate paint with glycerin.

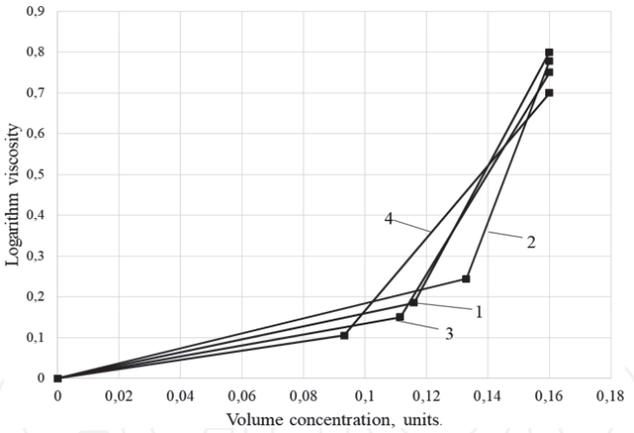

Figure 8.
The dependence of viscosity on the volume fraction of pigment in the coordinates lgη- C*: (1) red iron oxide; (2) ocher; (3) ultramarine; (4) chromium oxide.*

The point of intersection projected on the x-axis will be the critical volume concentration of the pigment (CVCP) [4, 15].

As the results in **Figure 7** show, the viscosity of the paint increases during filling, while its change at low degrees of filling can be described by the Einstein equation:

$$\varphi = \varphi_O(1 + 2.5\varphi) \tag{11}$$

where η_0 is the viscosity of the unfilled system and φ is the volume fraction of the pigment (filler).

With increasing concentration of the dispersed phase (more than 0.08), the interaction between particles increases, and deviations from the Einstein equation have been detected. These deviations are apparently due to the interaction of the particles and the formation of a structure in which the particles of the dispersed phase are oriented relative to each other in a certain way (structuring systems). The results of the calculations show that the model changes the viscosity of the paint from the volume concentration of the pigment (filler) which can be described by a polynomial

$$\eta = \eta_o(a + b\varphi + c\varphi^2 + d\varphi^3) \tag{12}$$

where η_0 is the viscosity of the unfilled system and φ is the volume fraction of the pigment (filler).

The following equations were obtained:

$$\eta = \eta_o(0.334 + 119\varphi - 2110.47\varphi^2 + 12217.83\varphi^3) \text{–for sol silicate paint} \tag{13}$$

Testing the adequacy of the model showed that Eq. (2) is valid in the filling region up to φ = 0.16.

In view of the foregoing, the cohesive properties and the ability of the polysilicate binder to wet the surface of the pigment (filler) were also investigated. In the work, polysilicate solutions were obtained by the interaction of stabilized solutions of colloidal silica (sols) with aqueous solutions of alkaline silicates (liquid glasses). A sodium liquid glass with a modulus M = 2.78 was used, and a potassium liquid glass with a modulus M = 3.29.

We was calculated the work of adhesion of liquid glass and polysilicate solution to the pigment (filler). The contact angle of wetting was determined on the KRUSS DSA-30 [13].

To determine the wetting contact angle, tablets are mixed from the mixture of pigment and filler with the automatic hydraulic press Vaneox-40 t, with a pressure of 18 tons for 11 seconds. The powder compressed in a dry state, without further processing. The surface tension of the solutions is determined by the stalagmometric method. The stalagmometric method based on measuring the number of droplets formed when a liquid flows out of a vertical tube of a small radius.

Analysis of the data (**Table 1**) shows that for the potassium polysilicate solution, a large work of adhesion to the filler (pigment) is characteristic. Thus, the work of adhesion of the potassium polysilicate solution to the filler (pigment) is 103.85 mN/m, while the work of adhesion of potassium liquid glass is 87.74 mN/m. Similar regularities are observed when using sodium liquid glass and sodium polysilicate solution. A potassium polysilicate solution is also characterized by a large wetting work of 39.786 mN/m.

In determining the wetting contact angle, it was found that sodium glass droplets on the surface of the sample formed an angle much larger than that of the potassium and for 5 minutes remained unchanged on the surface, while the drops from the potassium for half a second remained in shape and then blurred. Drops based on the sodium polysilicate solution were quickly absorbed into the material, forming a pyramidal shape. Drops based on the potassium polysilicate solution are more stable and retained on the sample for up to 2 minutes.

The availability of more complete wetting of the surface of the filler and the pigment in the case of the use of a potassium polysilicate solution promotes the formation of a denser coating structure and an increase in the physicomechanical properties. This is evidenced by data on the change in the tensile strength of films based on colorful compositions.

It was found that the cohesive strength of membranes based on sol silicate paint is 2.65 MPa and based on silicate paint 1.8 MPa (**Figure 9**). An increase in the relative deformations is observed, which is 0.06 mm/mm for membranes based on sol silicate paint and 0.033 mm/mm based on silicate paint.

In continuation of further research, frost resistance tests were carried out by alternate freezing and thawing painted mortar samples. The samples were painted with silicate and sol with silicate paint with intermediate drying for 20 minutes. After the coatings were cured, frost resistance tests were carried out. Evaluation of the appearance of the coatings was carried out according to GOST 6992-68 "Paint coatings. Test method for resistance to atmospheric conditions". The status of coating, assessed as AD3 and AZ4, was taken as a "failure" [7]. The energy of interaction between particles of the coating was estimated by value of the Hamaker constant [16]. It was established that the condition of the coating based on silicate

Name of film-forming	Surface tension, mN/m	°Angle of wetting, °	Adhesion work, mJ/m^2	Wetting operation, mN/m
Water	72.8	46.2	123.18	50.38
Binder				
Potassium liquid glass	55.22	53.9	87.74	32.52
Potassium polysilicate solution (15% Nanosil 20)	64.064	51.6	103.85	39.786
Sodium liquid glass	51.66	74.7	65.3	13.64
Sodium polysilicate solution (15% Nanosil 20)	55.22	62.5	80.73	25.51

Table 1.
The work of adhesion of a polysilicate binder to a filler.

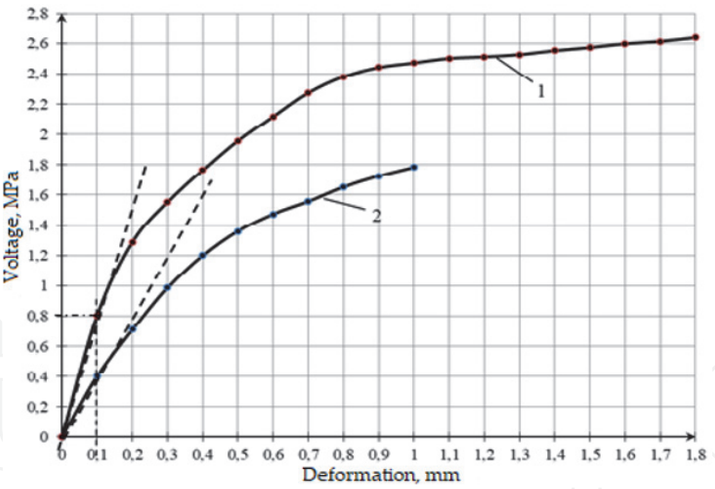

Figure 9.
Change in the relative deformations when tensile samples based on: (1) sol silicate paint; (2) silicate paint.

paint after 35 cycles is estimated as AD1 and AZ1, which corresponds to the state of coating with no discoloration, chalking, and dirt retention. Silicate-based coatings are more susceptible to degradation. The condition of coating based on silicate paint is estimated as AD3 and AZ3. The test results showed that the "failure" of coating based on silicate paint occurred after 40 freeze-thaw cycles, while the state of the coating based on polysilicate solution was evaluated as AD2 and AZ2. The "failure" of the coating based on the polysilicate solution occurred after 50 test cycles. Adhesion strength after 50 test cycles in accordance with GOST 31149 "Paint and varnish materials. Determination of adhesion by the lattice cut method" for silicate coatings and for coatings based on polysilicate solution was by 1 point.

The surface energy of the coatings was calculated using the critical surface tension of the liquid at the boundary with a solid (method of Zisman). The dispersion contribution to the intermolecular interaction between the particles of the coatings was estimated, for which the value of the complex Hamaker constant A* was additionally determined, which takes into account the complex action of the two components—the interparticle interaction between homogeneous particles and the interfacial interaction at the solid-solution interface.

The measurement data of the contact angle showed that for all samples studied, a linear dependence $\cos\theta = f(\sigma_{lig})$ is observed (**Figure 9**). By extrapolating the dependence $\cos\theta = f(\sigma_{lig})$ by $\cos\theta = 1$, we obtained value of the critical surface tension of a solid surface (coating). The energy of interaction between particles of the coating was estimated by value of the Hamaker constant calculated by the equation

$$\cos\theta - 1 = \frac{A^*}{12h_{\min}\sigma_{ж}} \tag{14}$$

where h_{min} is the smallest membrane thickness, which corresponds to the van der Waals distance (0.24 nm); $\sigma_{ж}$ is the surface tension of the liquid; and A* is the complex constant of Hamaker in interaction of a liquid with a solid at the boundary with air.

To calculate the complex Hamaker constant, functional dependences $\cos\theta\text{-}1 = f(1/\sigma_{lig})$ were built. **Figures 10–12** present results for coatings based on silicate and sol silicate paints [17].

Table 2 presents the calculated values of the surface tension of coatings and the Hamaker constant A*.

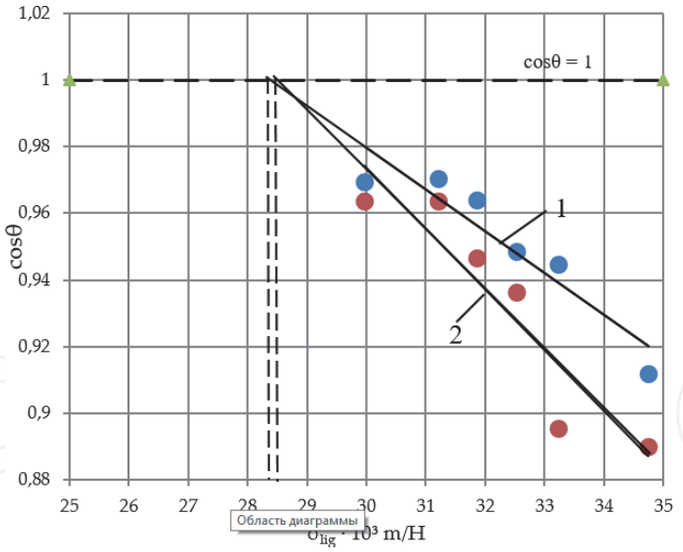

Figure 10.
The dependence cosθ = f (σlig): (1) on coating based on silicate paint; (2) on coating based on sol silicate.

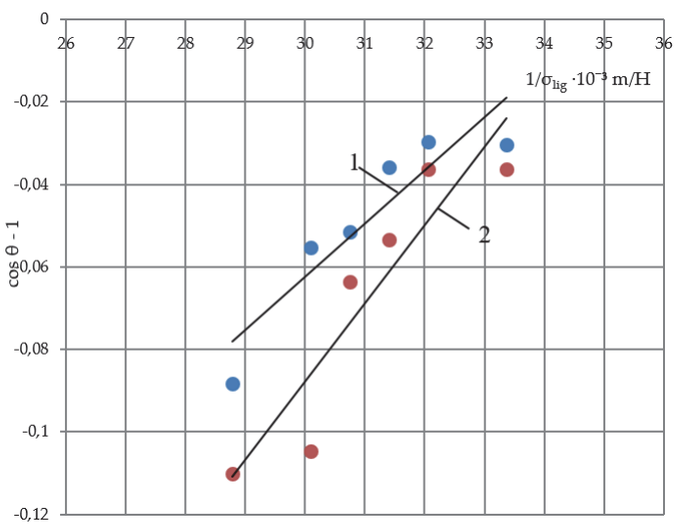

Figure 11.
Functional type dependency cosθ-1 = f (1/σlig) before testing coatings based on: (1) silicate paint; (2) sol of silicate paint.

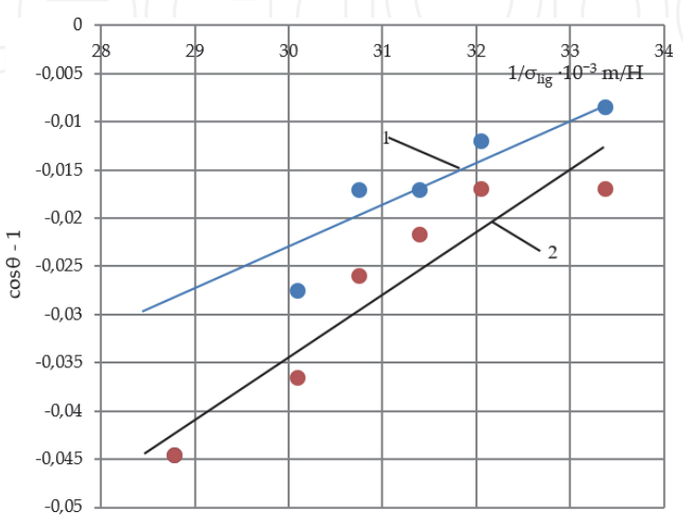

Figure 12.
Functional dependence of the form cosθ-1 = f (1/σlig) after 50 test cycles of coatings based on: (1) silicate paint; (2) sol of silicate paint.

Type of paint coating	Value critical surface tension of the coating [mN/m]	Constant value Hamaker A*10^{-20} [Дж*]
Based on potassium liquid glass	28.4	2.85 1048
Based on potassium polysilicate solution	28.7	4.09 1524

**Above the line is the value of the Hamaker constant for coatings prior to frost resistance test, below the line—after the test.*

Table 2.
Surface tension values of silicate coatings.

Name indicators	Values
Portability	Good
Class of quality of appearance of coatings	IV
Viscosity to B3-4 [s]	17–20
Shrinkage, the presence of cracks	No
Viability [day]	More 90
Drying time [minute], to degree 5	15–25
Adhesion [points]	1
Adhesion [MPa]	1.1–1.3
Coefficient of vapor permeability [mg/m × hPa]	0.00878
Relative hardness	0.47
Impact strength [kgcm]	50
Washability [g/m^2]	No more 2
Water resistance (appearance after 24 hours in water)	Absence of white matte spots, flaking, rashes, bubbles
Frost resistance, brand	F35

Table 3.
Properties of the paint composition and coatings based on it.

Analysis of experimental data shown in **Figures 10–12** indicates that the critical surface tension of the coatings is almost the same, which is apparently explained by the almost identical nature components of coating. The value of the Hamaker constant for coatings based on polysilicate solution, amounting to 4.09×10^{-20} J, is higher than the coatings based on silicate paints. This is confirmed by data on the higher strength of coatings based on polysilicate solutions. A higher value of the Hamaker constant for coatings based on polysilicate solution after frost resistance testing, equal to 1524×10^{-20} J, indicates a greater preservation of interparticle interaction in the coating.

Table 3 shows the values of the properties of coatings based on sol silicate paint.

4. Long-lasting durability of paint coatings

The temperature-time dependence of the strength of paint and varnish materials can be described by the Zhurkov Equation [18, 19]:

$$\iota = \iota_o \exp\left[(U_o - \gamma\sigma)/RT\right] \tag{15}$$

where γ is the structural-sensitive factor characterizing overstrain of bonds in the structure of the material; U_o is the activation energy of the process of destruction; R is the universal gas constant; and T is the absolute temperature.

The values of the activation energy of the fracture process and the structure-sensitive factor for polyvinyl acetate cement PVAC, organosilicon KO-168, and silicate coatings were calculated.

Figures 13–17 in semilogarithmic coordinates show the experimental dependence of the long-term cohesive strength of coatings from the value of tensions and temperatures for the coatings under study. The values of the structure-sensitive factor and the activation energy of the process of destruction of coatings are given in **Table 4.**

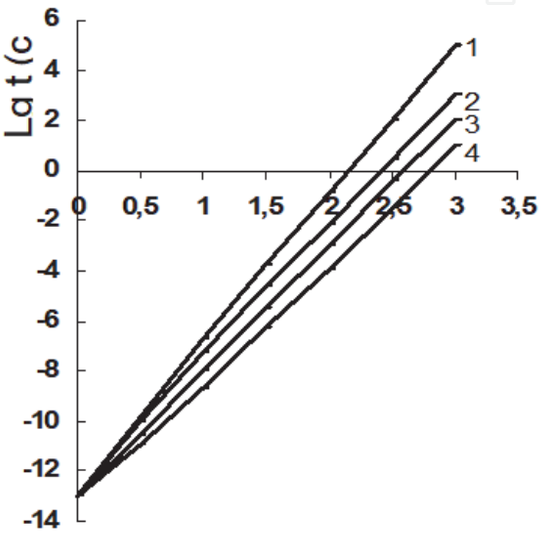

Figure 13.
The temperature dependence of lgτ *(σ): (1) coating of PVAC, σ = 0.166 MPa; (2) coating of PVAC, σ = 0.124 MPa; (3) coating of KO-168, σ = 0.144 MPa; (4) coating of KO-168, σ = 0.17 MPa.*

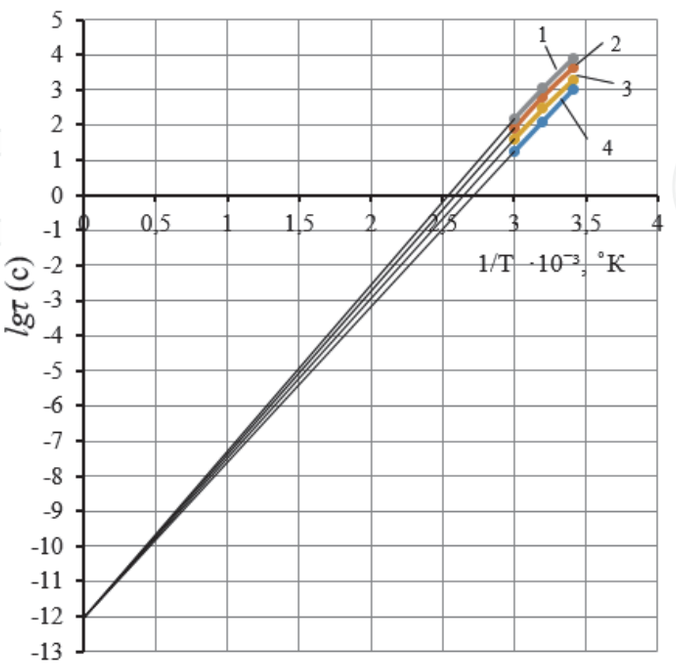

Figure 14.
The temperature dependence of coating based on silicate paint lgτ(σ): (1) stress σ = 0.14 MPa; (2) stress σ = 0.28 MPa; (3) stress σ = 0.42 MPa; (4) stress σ = 0.56 MPa.

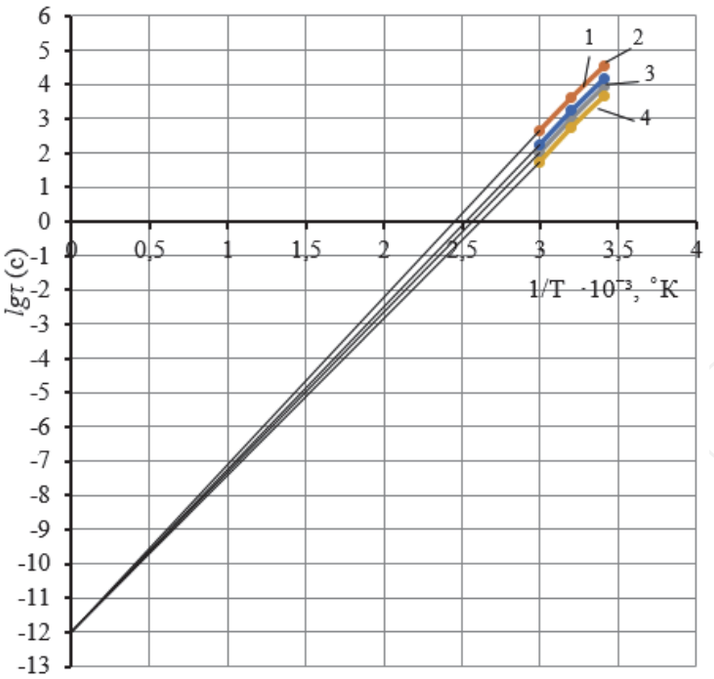

Figure 15.
The temperature dependence of coating based on sol silicate paint lgτ (σ): (1) stress σ = 0.14 MPa; (2) stress σ = 0.28 MPa; (3) stress σ = 0.42 MPa; (4) stress σ = 0.56 MPa.

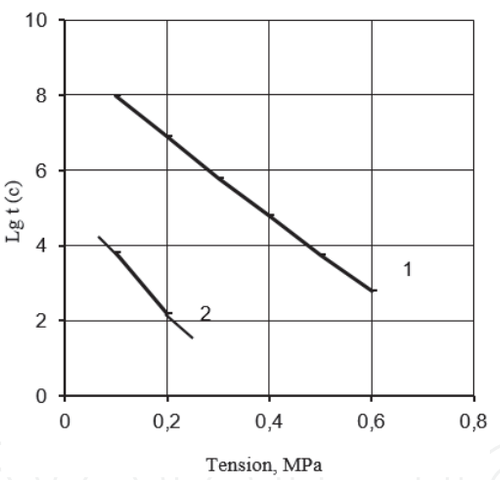

Figure 16.
Dependence of the long-term strength of coatings from tensions: (1) coating of PVAC; (2) coating of KO-168.

Analysis of the data in **Table 4** shows that the activation energy of cohesive destruction of coatings decreases with increasing stresses acting on the coatings. A higher value of the activation energy and a lower value of the structurally sensitive factor indicate high strength of polyvinyl acetate cements compared with organosilicon coatings.

The duration of maintaining the cohesive strength of coatings during operation is also determined by the resistance to periodic exposure to environmental factors: wetting, drying, freezing, thawing, etc. It was determined the change in cohesive strength as a function of wetting time. To this end, stretched film samples were sprinkled.

The duration of preservation of cohesive strength of coatings during operation is also determined by the resistance to periodic effects of environmental factors: wetting-drying, freezing-thawing, etc. In this connection, the influence of humidification on the change in the duration of cohesive strength was assessed. To this

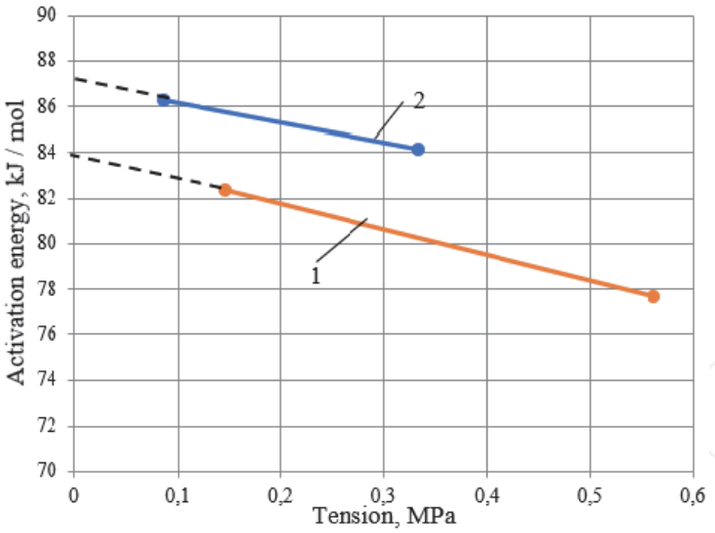

Figure 17.
Values of the activation energy of the process of destruction of coatings depending on tensions: (1) coating based on silicate paint; (2) coatings based on sol silicate paint.

Type of coating	U_o	γ
Polyvinyl acetate cement	122.81	27.98
Silicone KO-168	102.53	42.86
Silicate	84	11.14
Sol silicate	87	8.55

Note: For coatings $\iota_o = 10^{-13}$ s.

Table 4.
The values of U and γ of coatings.

end, stretched coating samples were subjected to sprinkling. The results of the tests are shown in **Figure 18**.

Consider the condition of brittle cracking of polymer coatings under investigation under the action of internal tensions. In the case of brittle failure, the cracking condition has the form

$$\sigma \geq 0.5R \tag{16}$$

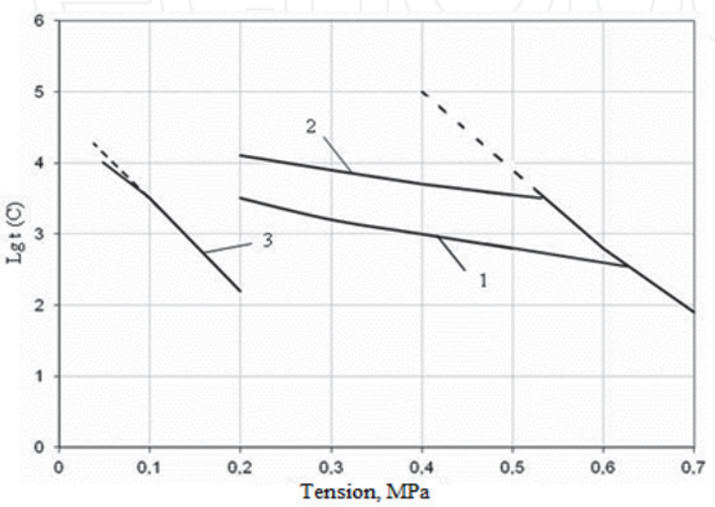

Figure 18.
Dependence of the long-term strength of coatings in the process of humidification: (1) coating of PVAC; (2) coating of PVAC with surface hydrophobization; (3) coating of KO-168.

Name of coatings	Internal stresses, MPa	Cohesive at strength of coatings, MPa	σ/R	Time of occurrence cracks, day
PVAC	0.08	0.38	0.21	Not observed
Polymer-lime	0.062	0.13	0.47	27
Lime	0.075	0.09	0.9	30

Table 5.
Physicomechanical properties of coatings after moistening.

Consider the change in internal stresses and the strength of coatings in the aging process on the example of humidification. It was found that at the first instant, humidification, a sharp increase in internal stresses, and then their slow decrease, i.e., an effect of the time factor, are observed. For example, for PVAC coatings, stabilization of internal stresses on level σ = 0.08 MPa is observed after 20 days of moistening, and stabilization of internal stresses in polymer-lime coatings is observed after 18 days of humidification on level σ = 0.062 MPa. The value of short-term strength after 60 days of moistening is given in **Table 5.**

The polyvinyl acetate cement coating after 2 months of moistening did not have cracks; the ratio σ/R for such coatings does not exceed 0.21.

Consider the kinetics of changes in the short-term strength of coatings during aging from the perspective of the kinetic concept of the strength of solids. It is known that the number of structural bonds N determines the strength of a material

$$R = f(N) \tag{17}$$

During operation, there is a change in the number of structural bonds.

$$n_1 u_o = \gamma\sigma \tag{18}$$

where u_0 is the unit bond breaking energy and γ is the structurally sensitive coefficient, characterizing the overvoltage of bonds.

The state of the material structure at a time t_1 is characterized by the value of the activation energy of bond breaking:

$$U_t = U_o - \gamma\sigma = U_o - n_1 u_o \tag{19}$$

The increase in the number of severed bonds at time due to the increase dU will be equal to

$$dn_1/N_o = \alpha dU \tag{20}$$

Integration of Eq. (20) leads to the form

$$n_1 = N_o \exp(-\alpha N_1) \tag{21}$$

In view of Eq. (18),

$$n_1 = N_o \exp[-\alpha(U_o - \gamma\sigma)] \tag{22}$$

During long-term operation, short-term strength is reduced in proportion to the number of broken bonds n_1:

$$R_t/R_o = [(N_o - n_1)/N_o] : [(\tau - t)/\tau] \tag{23}$$

where τ is the durability of the coating and t is the operating time.

After the transformation, Eq. (23) has the form

$$R_t = \{R_o\tau \exp(U/RT)[1 - \exp(-\alpha U)]\}/(\tau_o \exp(U/RT)) - t \quad (24)$$

Thus, the cracking condition has the form

$$\sigma_{\max} = 0.5\{R_o\tau \exp(U/RT)[1 - \exp(-\alpha U)]\}/(\tau_o \exp(U/RT)) - t \quad (25)$$

The obtained cracking condition (25) was used in the analysis of coating cracking due to wind load.

Consider the work of the coating in the pore zone, unfilled with a colorful composition. Suppose that the distance with pores that are not filled with a colorful composition is larger than the size of the pores themselves. Such a coating can be considered as a thin round plate pivotally supported along the contour, while the load is evenly distributed over the area. The coating thickness does not exceed 1/5 of the smallest pore size. The calculations established that the deflection boom does not exceed 1/5 of the coating thickness; therefore, such a plate can be considered rigid.

In accordance with the theory of plates, the magnitude of the stresses arising in the coatings can be determined by the formula

$$\sigma = \left(1.5 - 0.262\alpha^2 - 1.95\ln\alpha\right)q(d/h)^2 \quad (26)$$

Name cities	Floor	Tension, $\sigma \cdot 10^{-1}$ MPa					
		Pore diameter, mm					
		0.1	0.2	0.5	1.0	2.0	3.0
Moscow	1–2	0.01	0.03	0.18	0.71	2.85	6.41
	3	0.01	0.01	0.11	0.44	1.77	4.00
	6	0.01	0.04	0.23	0.93	3.73	8.33
	12	0.01	0.02	0.14	0.57	2.31	5.20
		0.01	0.05	0.30	1.21	4.84	10.89
		0.01	0.03	0.18	0.75	3.00	6.80
		0.02	0.06	0.39	1.57	6.26	14.09
		0.01	0.03	0.24	0.96	3.86	8.70
Penza	1–2	0.01	0.04	0.23	0.93	3.71	8.36
	3	0.01	0.02	0.14	0.58	2.32	5.22
	6	0.01	0.05	0.30	1.21	4.83	10.86
	12	0.01	0.03	0.18	0.75	3.01	6.78
		0.01	0.06	0.39	1.58	6.31	14.21
		0.01	0.04	0.24	0.99	3.94	8.87
		0.02	0.08	0.51	2.04	8.17	18.38
		0.01	0.05	0.39	1.27	5.10	11.49
Vladivostok	1–2	0.02	0.07	0.46	1.86	7.43	16.76
	3	0.01	0.04	0.29	1.16	4.64	10.40
	6	0.02	0.1	0.6	2.41	9.66	21.73
	12	0.01	0.07	0.45	1.83	7.34	16.50
		0.03	0.13	0.79	3.16	12.63	28.41
		0.01	0.08	0.49	1.97	7.89	17.70
		0.04	0.16	1.02	4.09	16.34	36.77
		0.01	0.1	0.63	2.55		22.90

Note: Above the line are voltage values for PVAC coatings with a thickness of 200 μm and below the line for coating XB-161 with a thickness of 80 μm.

Table 6.
Tensions in coatings due to wind load.

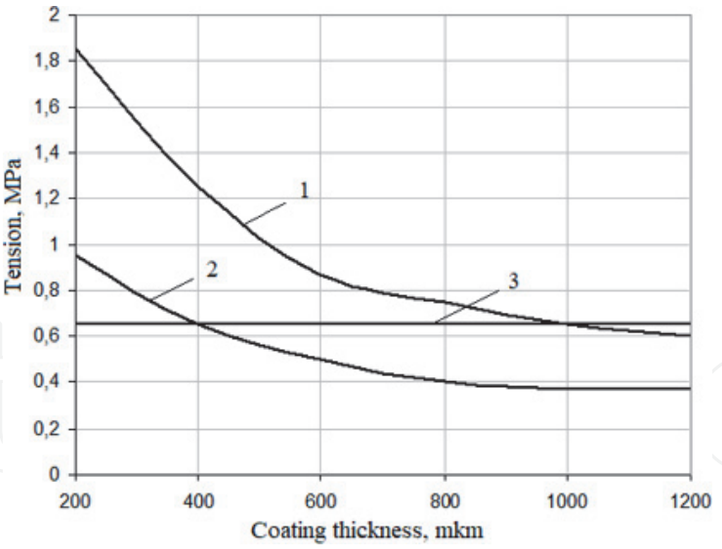

Figure 19.
Choosing the optimal coating thickness taking into account the duration of the voltage: (1) current voltage; (2) short-term strength; (3) long-lasting strength.

where h is the coating thickness; d is the pore diameter; and q is the load.

The external wall self-supporting panel of the building experiences the effect of horizontal wind load. In accordance with SNiP 2.01.07 "loads and impacts," the normative value of the average component of the wind load was selected. The results of calculating the stresses arising in thin-coat paint coatings during operation from the action of the wind load are given in **Table 6**.

Given the influence of the scale factor and the condition of brittle fracture of the coatings, the optimum coating thickness was selected (**Figure 19**).

Line 1 characterizes the numerical values of the acting tensions. Curve 2 characterizes the change in the short-term strength of PVAC coatings from the coating thickness in accordance with Eq. (21). Since the coating is in a brittle state, the steady-state long-term strength for each thickness is 0.5 of the short-term, i.e., curve 3.

An analysis of the data, (**Figure 19**), indicates that under the short-term effect of the wind load, destruction of the PVAC coatings will occur when the coating thickness is more than 850 μm, since for them $\sigma > 0{,}5\,R$ with long exposure to wind load, destruction will occur at a thickness of 300–850 μm. Coatings less than 300 microns thick are resistant to cracking, as $\sigma < R$ and $\sigma < 0{,}5\,R$. Each type of coating has its own critical pore size, exceeding which leads to cracking of the coatings.

5. Conclusion

The received results of research of a roughness of a surface of coverings confirm the assumption that quality of a substrate, namely, the degree of its uniformity, presence or absence of pollution on its surfaces, and its porosity render essential influence on quality of appearance of formed coverings that determines their stability while in service.

Studies have been conducted to evaluate the long-term strength of coatings. The values of the structurally sensitive factor are calculated. The condition for coating cracking is obtained, depending on the activation energy and operating time. Given the influence of the scale factor and the conditions for the destruction of coatings, a methodology is proposed for selecting the optimal thickness of the coatings. It is established that for each type of coating, there is a critical pore size, exceeding which leads to cracking of the coatings.

Author details

Valentina Loganina* and Yerkebulan Mazhitov
Penza State University Architecture and Construction, Penza, Russia

*Address all correspondence to: loganin@mail.ru

IntechOpen

References

[1] Loganina VI, Orentlikher LP. Persistence of Protective and Decorative Coatings of the Exterior Walls of Buildings. Moscow: Publishing House Association of Construction Universities; 2001. p. 104

[2] Orentlicher LP, Loganina VI. Protective and Decorative Coatings of Concrete and Stone Walls. Handbook. Moscow: Stroyizdat; 1993. p. 136

[3] Andrianov KA. Organosilicon Compounds. Goskhimizdat: Moscow; 1995. p. 234

[4] Karyakina MI. Physico-Chemical Foundations of the Formation and Aging of Coatings. Moscow: Chemistry; 1980. p. 216

[5] Sukhareva LA. The Durability of Coatings. Moscow: Chemistry; 1984. p. 240

[6] Loganina VI. Durability of paint and varnish coatings depending on the quality of their appearance. IOP Conference Series: Materials Science and Engineering. 2016;**471**:022044

[7] Andryushenko EA. Lightfastness of Paint and Varnish Coatings. Moscow: Chemistry; 1986. p. 187

[8] Bartenev GM, Zuev YS. Strength and Destruction of Highly Elastic Materials. Moscow-Leningrad: Chemistry; 1984

[9] Loganina VI. The influence of surface quality of coatings on their deformation properties. Contemporary Engineering Sciences. 2014;7(36): 411241

[10] Bykhovsky AA. Distribution. Kiev: Science, Dumka; 1983. p. 191

[11] Loganina VI, Skachkov Yu P. Assessment of the stress state of the coating in depending on the porosity of the cement substrate. Key Engineering Materials. 2016;**737**:179-183

[12] GOST R 8.700–2010. State system for ensuring the uniformity of measurements. Methods of surface roughness effective height measurements by means of scanning probe atomic force microscope

[13] Zisman GA, Todes OM. The Course of General Physics. Moscow: Chemistry; 1968

[14] Loganina VI, Kislitsyna SN, Mazhitov Ye B. Development of sol-silicate composition for decoration of building walls. Case Studies in Construction Materials. 2018;**9**:e00173

[15] Gurevich MM, Itsko EF, Seredenko MM. Optical Properties of Paint Coatings. Leningrad: Chemistry; 1984. p. 120

[16] Ajzenshtadt AM, Frolova MA, Tutygin AS. Fundamentals of Thermodynamics of Highly Dispersed Systems of Rocks for Building Composites (Theory and Practice). Arkhangelsk: CPI NarFU; 2013. p. 113

[17] Loganina VI, Mazhitov YB. Research of inter-phase interaction in ZOL-silicate paints. International Journal of Engineering & Technology. 2018;7(4.5): 605-607

[18] Zhurkov SN, Narzulaev BN. Temporal dependence of solids. Journal of Technical Physics. 1953;**23**:1677

[19] Bokshitsky MN. Long-Lasting Polymer Strength. Moscow: Chemistry; 1978. p. 309